Adsorption properties of lignin containing bentonite–polyacrylamide composite for UO_2^{2+} ions

Selçuk Şimşek

Faculty of Sciences, Department of Chemistry, Cumhuriyet University, Sivas, Turkey, Tel. +90 346 219 1010, ext. 2139; email: simsek@cumhuriyet.edu.tr

ABSTRACT

As a new material, a composite of polyacrylamide (PAA)-Bentonite (B) containing Lignin (L) was synthesized and adsorption properties of this new material was studied for the removal of uranyl ions from solution. The material was characterized by Fourier transform infrared spectroscopy, scanning electron microscopy, X-ray diffraction, and PZC analysis. The effects of experimental variables such as concentration, pH, ionic strength, temperature, and kinetic of adsorption were investigated. The adsorption data were analyzed using the Langmuir, Freundlich, Temkin, and Dubinin–Radushkevich (DR) equations. The adsorption process is evaluated with pseudo-first-order, pseudo-second-order, Elovich, and intraparticle diffusion models. The Q_L (mol kg^{-1}) and K_L (L mol^{-1}) values for adsorption from solution were 0.314 and 1,321 for PAA-B-L. This investigation showed that the new developed material can be used for the removal of UO_2^{2+} ions from aquatic solutions.

Keywords: Uranyl; Lignin; Adsorption; Composite; Bentonite

1. Introduction

Uranium is a useful element in industry with radiological and chemical properties but it has health risks for humans, particularly at relatively high concentrations because of its chemical toxicity and radioactivity. The hexavalent uranyl ion (UO_2^{2+}), the most common form of uranium in aqueous solution, can bond with chelating agents such as citrate, bicarbonate anions, and plasma proteins in blood [1]. It can accumulate in organs and cause several health problems. The tolerable daily intake of uranium is established as 0.6 µg kg^{-1} of body weight [2]. Therefore, the removal and recovery of uranium in aqueous medium are one of serious concerns due to their toxic and radioactive properties.

The adsorption is generally known to be one of the most effective techniques for the removal of uranyl ions among several techniques such as precipitation [3], ion exchange [4], and extraction [5]. It is not only a removal method, but it is also used for enrichment, recovery, and pre-concentration of uranium due to simplicity, relative selectivity, efficiency, practical use, and low cost [6–8]. Several materials such as clay [9,10], natural or synthetics polymers [11–13], and composites [14,15] have been used as adsorbent for the removal of uranyl ions.

Lignin (L) is a natural polymer existing in the cell walls of plants and approximately 50 million tons of lignin is generated annually by the paper industries all over the world, but less than 10% of it is utilized. It is

also a chelating agent for metals due to its three-dimensional amorphous structure and functional groups in its structure such as phenolic, hydroxyl, carboxyl, methoxyl, and aldehyde groups [16]. Depending on source and functional groups, lignin can exist in kraft or sulfonated forms. Sulfonated form is particularly a potential adsorbent with $-SO_3H$ groups for the removal of metals but it is not used for adsorption process due to its solubility in water. If it could be immobilized or entrapped in matrix by chemical or physical modification then it can be used as potential adsorbent [17].

Bentonite (B) is clay of the smectite group and is used as an adsorbent for the removal of metals and organic pollutants such as pesticides, phenolic compounds, and dyes in water [18,19]. However, its practical use in metal adsorption is limited due to coagulation and gel-like sticky material that forms when it interacts with water. Our previous study showed that the composite of B and PAA is an effective adsorbent for uranyl ions in aqueous medium [20].

The main advantages of newly developed material can be summarized with a few sentences. Raw materials of new composite are cheap, accessible, and natural. Lignin is known as a waste of paper industry and bentonite is already an easily available natural mineral. The developed material has both high absorption capacity and contains environmentally friendly components. This study investigated a new lignin-based material, polyacrylamide–bentonite-lignin (PAA-B-L) and the adsorption properties of this new material for the removal of UO_2^{2+} in aqueous solution. The Fourier transform infrared spectroscopy (FTIR), scanning electron microscopy (SEM), X-ray diffraction (XRD), and point zero charge (PZC) analysis were performed. Experimental variables such as uranyl concentration in solution, pH, ionic strength, time, and temperature were studied. Results have showed that PAA-B-L could be used successfully for the removal of UO_2^{2+} from water samples.

2. Experimental

2.1. Reagents

All chemicals which were used were of analytical reagent grade. Bentonite (98% purity), acrylamide (AA) monomer, N,N′-methylenebisacrylamide (Bis–AA), N,N,N,N-tetramethyl ethylenediamine (TEMED), and 4-(2-pyridylazo) resorcinol (PAR) were purchased from Sigma (St. Loius, MO, USA). Sulfonated lignin was supplied by MeadWestvaco Corp. (USA). UO_2 $(NO_3)_2\cdot6H_2O$ and the remaining chemicals were obtained from Merck (Germany). The experiments were always performed in duplicate.

2.2. Preparation of PAA-B-L

Two grams of Bentonite in 50 mL of distilled water and 2 g of Lignin were stirred for 30 min using a magnetic stirrer. 10 mL of solution containing 4 g of acrylamide monomer was added to the suspension to provide polymerization and it was stirred for additional 30 min. Polymerization was started using 100 µL of N,N,N′,N′-tetramethylethylenediamine at 298 K. Finally, PAA-B-L composite was obtained through adding the propagating reagent. The composite sample was dried at ambient temperature, ground, and sieved to a particle size smaller than 1 mm, and stored in a polypropylene container.

2.3. Point of zero charge and pH dependence of adsorption

The acidic–basic character of adsorbent was investigated and the PZC was measured in order to determine the charge of surface. For this purpose, 0.1 g of adsorbent was interacted with 0.1 mol L^{-1} KNO$_3$ solutions having initial pHs in the range of 1–14 for 24 h at 298 K. The diluted NaOH and HCl were used for the pH adjustments. The final pHs of solutions were measured using a pH meter.

2.4. Adsorption studies

Adsorptive features of PAA-B-L were studied for UO_2^{2+} ions. For this purpose, 0.1 g of the adsorbent was equilibrated with 10 mL of UO_2^{2+} in the concentration range of $(0.19–5.5) \times 10^{-3}$ mol L^{-1}. The adsorbent–solution systems were equilibrated for 24 h at 298 K and equilibrium was obtained by centrifuging for 5 min.

The concentration of uranyl ions was determined using modified PAR method by UV–vis spectrophotometer (Shimadzu, Japan) [21]. In this method, uranyl ions form a selective complex with PAR (4-(2-pyridylazo) resorcinol) at pH 8.5, and 3.5×10^{-3} mol L^{-1} of PAR was prepared in Tris/HCl buffer (pH 8.5, 0.7 mol L^{-1}). A fraction of supernatant, 500 µL, was added onto 3 mL of the reagent, and the absorbance of the formed complex was measured at 530 nm.

3. Results and discussion

3.1. Structural evaluation

The FTIR analyses were studied using FTIR spectrophotometer (Inter-spec 2020, spectrolab, UK) in KBr pellets. The FTIR spectra of B, PAA, and L are given in Fig. 1. The detailed analyses of these structures were given in our previous studies. The FTIR
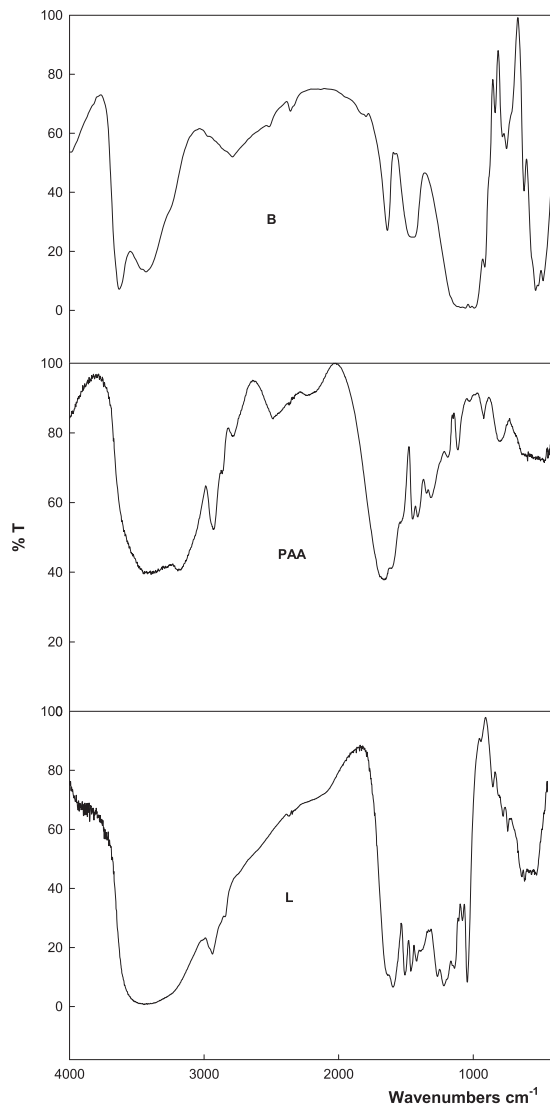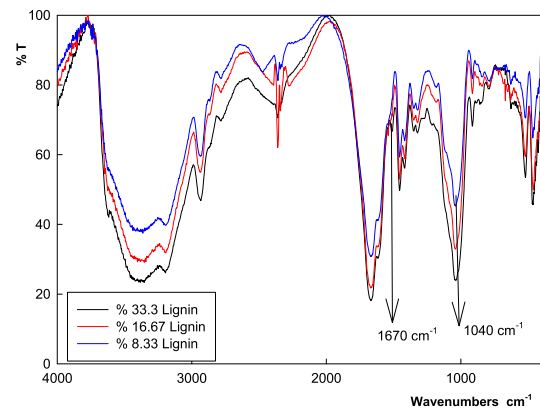
Fig. 1. FTIR Spectra of B, PAA and L.

Fig. 2. FTIR Spectra of PAA-B-L containing different mass ratio of lignin (lignin content: Blue: 8.33%, Red: 16.67%, Black: 33.33%).

increasing amount of Lignin was an evidence for L penetrated the PAA-B structure.

XRD (Rigaku smart lab, high resolution, using Cu K_α radiation, 45 kV, 50 A, λ 1.54059 Å) was used for powder diffractions of B, PAA-B, and PAA-B-L (Fig. 3). Bentonite was characterized with the diffractions appeared 12.45 and 4.48 Å at 7.1 and at 19.8 (2θ), respectively [26]. After the treatment of B with PAA and L, the basal spacing increased for PAA from 12.45 to 13.09 and for L to 13.70 Å. The increase in the basal spacing of PAA-B and PAA-B-L can explain the penetration of PAA and L. On the other hand, the FWHM (full width at half maximum) increased in XRD spectrum of PAA-B and PAA-B- L according to B. This should be the evidence for the existence of PAA and L in PAA-B and PAA-B-L as a result of deformation of layered structure of B.

The surface morphology of B, PAA-B, and PAA-B-L adsorbent (Fig. 4) was analyzed by SEM (LEO-450,

spectrum of B showed that the specific peaks of B were observed at 470–530 and 1,140−960 cm^{-1} of the Si–O, near 3,650 cm^{-1} of the O–H stretching bands of the surface silanol and 808 cm^{-1} of Al–O–H of B [20]. The spectrum of PAA showed a broad band of NH$_2$ at 3,600 cm^{-1}, peaks of carboxyl and amide groups (CONH$_2$) at 1,600–1,700 cm^{-1}, and a C–N stretch at 1,000–1,200 cm^{-1} [22]. The FTIR spectrum of L included the following characteristics; a peak hydroxyl (aliphatic or aromatic) at 3,410–3,460 cm^{-1} C–H of methyl and aromatic components at 2,840–3,000 cm^{-1} and R–SO$_2$–O$^-$ at 1,040–1,045 cm^{-1} [23–25].

The FTIR spectra of PAA-B-L which are different mass ratio of L were shown in Fig. 2. The increase of sharpness of peak at 1,040 and 1,670 cm^{-1} with the
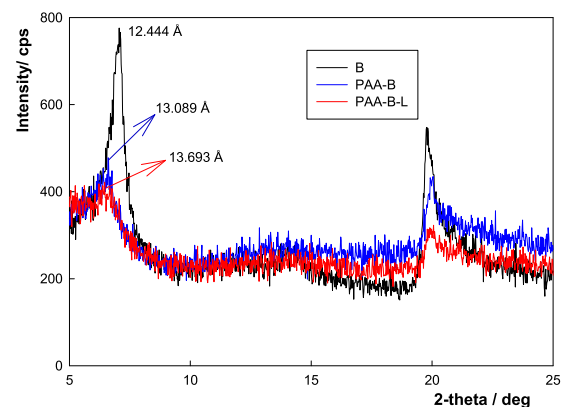

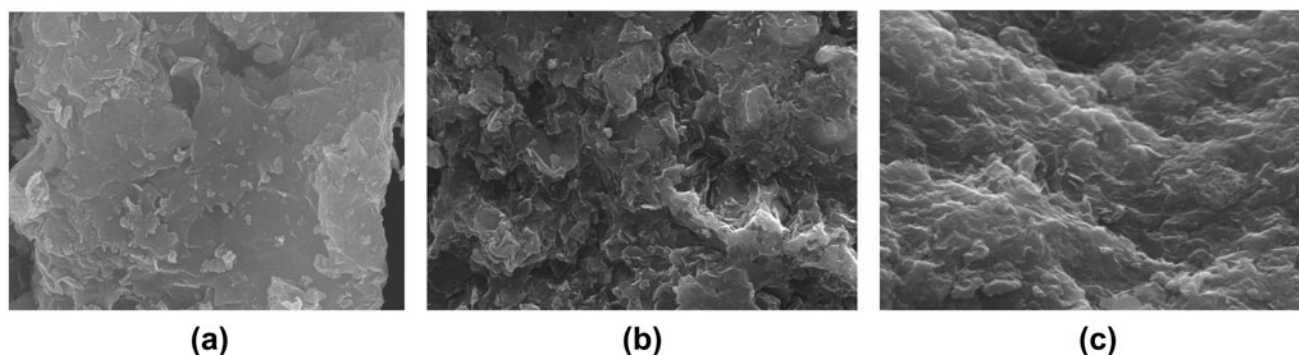Fig. 3. XRD Spectra of B, PAA, and PAA-B-L.

Fig. 4. SEM of views: (a) B, (b) PAA-B, and (c) PAA-B-L.

England). The surface morphology of PAA-B and PAA-B-L is obviously different from B. This difference shows that L could be successfully penetrated to PAA-B.

3.2. Effect of pH on UO_2^{2+} adsorption and determination of point zero charge

The pH of the aqueous solution is an important parameter in the adsorption process. The solution pH significantly affects the ionization degree of metals such as ionic species and the charges of adsorbent's surface via ionization of functional groups [24,27]. It depends on the extent of metal precipitation and the type of complexes formed metals in aqueous solution [28].

The effects of pH on UO_2^{2+} ($7.4 \times 10{-}3$ mol L^{-1}) adsorption by PAA-B-L were studied and the results were presented in Fig. 5. The results showed that the adsorption increased with pH. The values above pH 7.0 have not been over passed due to hydroxide precipitates of the UO_2^{2+} ion such as $UO_2(OH)_2$,

$UO_2(OH)_3^-$, $UO_2(OH)_4^{2-}$, $(UO_2)_3(OH)_7^-$, $(UO_2)_3(OH)_8^{2-}$, and $(UO_2)_3(OH)_1 1^{5-}$ [29].

The results showed that there was a competition between UO_2^{2+} and H^+ ions for the same donating atoms that caused a decrease in the adsorption at low pHs. The electron donor atoms of PAA-B-L such as carbonyl and hydroxyl groups exist in the protonated form at low pH values. The adsorption might increase in the presence of hydrolyzed uranyl species because the pH of the solution also affected the solubility of UO_2^{2+} at low pHs such as $[UO_2(OH)]^+$, $[(UO_2)_3(OH)_4]^{2+}$, $[(UO_2)_3(OH)_5]^+$, $[(UO_2)_3(OH)]^{3+}$, $[(UO_2)_4(OH)]_7^+$ [30].

The value of point of zero charge (PZC) was determined using (initial pH) pH_i and (final pH) pH_f (Fig. 6). The plateau of the $pH_i - pH_f$ plot corresponds to the pH range where the buffering effect of the PAA-B-L surface takes place [31]. The obtained plateau corresponds to pH_{pzc} from 4.0 to 11 for PAA-B-L. It means that for all values of pH_i, in this range, the pH_f equals to pH_{pzc}. The surface charge of PAA-B-L was positive at pH < 4, neutral between 4 and 11, and negative at pH > 11.
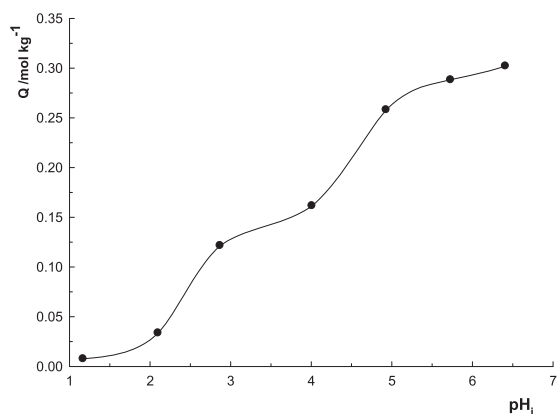

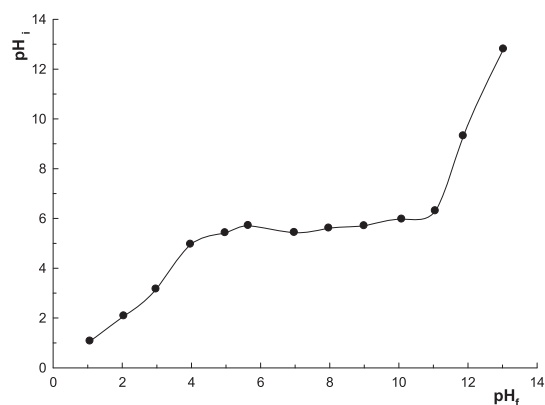Fig. 5. pH dependence of the adsorption.

Fig. 6. PZC plots of PAA-B-L.

The decreasing of UO_2^{2+} on PAA-B-L at low pH may be explained in terms of pH_{pzc} of PAA-B-L. The surface charge of PAA-B-L is positive at $pH < pH_{pzc}$. The electrostatic repulsion between UO_2^{2+} and positive surface of PAA-B-L becomes stronger at $pH < pH_{pzc}$.

3.3. Adsorption isotherms

The theoretical adsorption models such as Langmuir, Freundlich, DR, and Temkin models are commonly used for the evaluation of experimental results of adsorption. These models provide various parameters such as the surface properties, affinity of the adsorbent, and surface energy for adsorption [32–34].

The amounts of adsorbed UO_2^{2+} ions (Q, mol kg^{-1}) were calculated from the equation;

$$Q = \left[\frac{(C_i - C_e)V}{w} \right] \tag{1}$$

where C_i and C_e are the initial and equilibrium concentrations (mol L^{-1}), w is the mass of adsorbent (kg), and V is the solution volume (L). The different equilibrium adsorption isotherms were used to investigate experimental data as given in Table 1.

Uranyl adsorption experiments were applied to samples including lignin at three different concentrations in order to examine the effect of lignin concentration. For this purpose, the amount of lignin was

changed as 8.33, 16, 67, and 33.33%, while PAA and B concentrations are constant. As can be seen in Fig. 7, the capacity of adsorption increased by increasing lignin concentration as expected. The experimental variables such as temperature, time, pH, and ionic strength were investigated in detail and by considering this investigation, PAA-B-L including 33.3% lignin composite was selected due to its high adsorption capacity.

The adsorption isotherms of UO_2^{2+} and their compatibility to the Langmuir, Freundlich, DR, and Temkin models were compared in Fig. 8. Four isotherm constants as well as the coefficients of determination obtained by using the nonlinear method were presented in Table 2.

Among the isotherm models, Langmuir model provides two parameters like maximum adsorption capacities (Q_L) and a coefficient (K_L) attributed to the affinity between the sorbent and sorbets. K_L value, as a measure of adsorption affinity, made the superior affinity of UO_2^{2+} clear for PAA-B-L. This model suggested that the adsorption was homogeneous and monolayer [35]. The adsorption hyperbolically increases with increasing uranyl concentration. The steep rise in the beginning lowers gradually and reaches a plateau defining the completion of filling the monolayer adsorption capacity (Q_L).

Freundlich model was evaluated for adsorption of the heterogeneity of the adsorptive surface. The constant K_f is related to the degree of adsorption, and n provides the tentative estimation of the intensity of the adsorption [36]. The Freundlich parameter (n) was calculated as 0.261 for PAA-B-L and this indicated that UO_2^{2+} could be removed effectively from aqueous solutions.

Table 1
Mathematical equation of isotherm models

Model	Equation	Parameters
Langmuir	$Q_e = \frac{Q_L K_L C_e}{1 + K_L C_e}$	Q_L, K_L
Freundlich	$Q_e = K_F C_e^n$	K_F, n
Dubinin–Raduskevich	$Q_e = Q_{DR} e^{-K_{DR} \varepsilon^2}$	Q_{DR}, K_{DR}
Temkin	$Q_e = \frac{RT}{b} \ln(K_T C_e)$	B_T, K_T

Notes: Q_L: Langmuir monolayer adsorption capacity (mol kg^{-1}), K_L: Langmuir adsorption equilibrium constant (L mol^{-1}), K_F: Freundlich constants, n: Intensity of adsorption (n represents the heterogeneity of the adsorptive surface), K_{DR}: DR constant related to the sorption energy (mol^2 K J^{-2}), Q_{DR}: DR adsorption capacity (mol kg^{-1}), ε: Polanyi potential given with $\varepsilon = RT \ln \left(1 + \frac{1}{C_e}\right)$, R: Ideal gas constant (8.314 J mol^{-1} K^{-1}), T: absolute temperature (298 K), Free energy change (E; J mol^{-1}) required to transfer one mole of ion from the infinity in the solution to the solid surface was then derived from $E = (-2K_{DR})^{-1/2}$. $B_T = RT/b$, factor related to the heat of adsorption; K_T: Temkin equilibrium constant (L mol^{-1}).
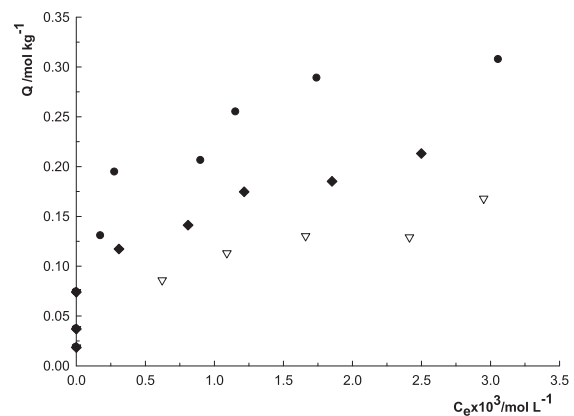

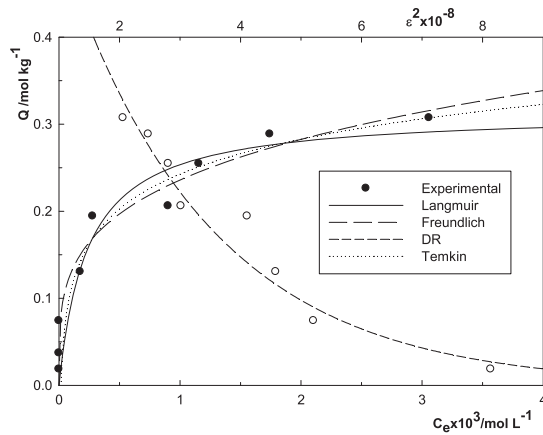Fig. 7. Effect of Lignin content on the adsorption of UO_2^{2+} (▽: 8.33% L, ◆: 16.67% L, ●: 33.33% L).

Fig. 8. Experimentally obtained adsorption isotherms UO_2^{2+} and their compatibility to Langmuir, Freundlich, DR, and Temkin models.

which suggested the Temkin constant, (B_T), shows that the heat of adsorption increases with temperature. This result shows that adsorption process is endothermic [40].

3.4. Effect of ionic strength

A series of experiments were carried out at constant UO_2^{2+} concentration $(3.7 \times 10^{-3} \text{ mol L}^{-1})$ by using various KNO_3 concentrations in order to follow the effect of ionic strength. As can be seen in Fig. 9, the amount of adsorbed UO_2^{2+} at equilibrium was not affected by increasing KNO_3 concentration. This result showed that the mechanism of adsorption is based on surface complex formation because it depends on pH of medium not ionic strength as explained in literature [41].

Table 2
Langmuir, Freundlich, DR, and Temkin parameters obtained for UO_2^{2+} adsorption on to PAA-B-L

	Parameters
Langmuir	
Q_L	0.314
K_L	1,321
R^2	0.892
Freundlich	
K_F	1.430
n	0.261
R^2	0.902
DR	
Q_{DR}	0.764
$-K_{DR} \times 10^9$	4.114
R^2	0.923
Temkin	
B_T	0.058
K_T	66,653
R^2	0.902
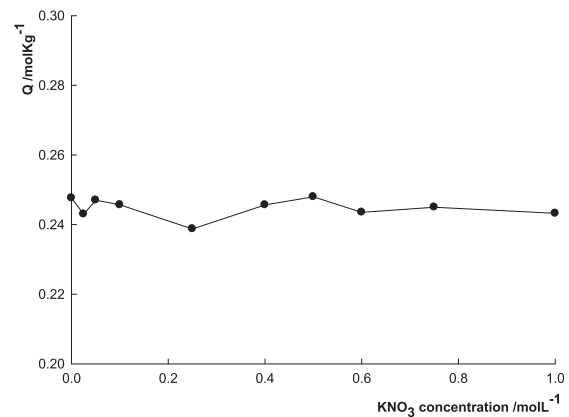
Fig. 9. Effect of salt concentration on the adsorption.
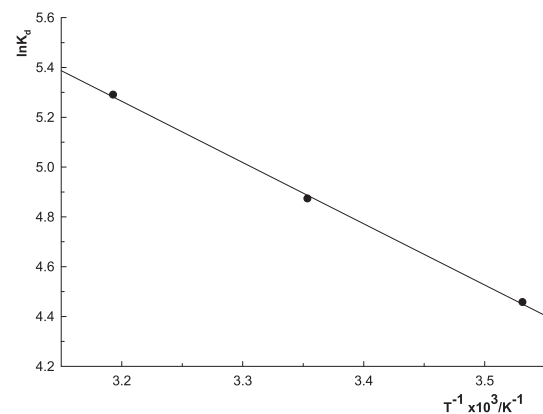
Fig. 10. Effect of temperature on the adsorption.

The experimental data fit to the DR isotherm very well with a high value of R^2 (0.923). The E_{DR} values suggest that the process was chemical adsorption [37] because the E value falls in the range from 8 to 16 kJ mol^{-1} and the physical forces such as diffusion process are effective on sorption if $E_{DR} < 8$ kJ mol^{-1} [38].

The Temkin isotherm assumes that the heat of adsorption decreases linearly while the coverage of adsorbent increases due to adsorption process [36,39]. The results were applied also to the Temkin model,

Table 3
Thermodynamic parameters for UO_2^{2+} onto PAA-B-L

$\Delta H°$/kJ mol^{-1}	$\Delta S°$/J mol^{-1} K^{-1}	$-\Delta G°$/kJ mol^{-1}	[a]R^2	E_{DR}/kJmol^{-1}
20.444	109.160	12.069	0.999	11.024

[a]Coefficients of variations for the linearity of ln K_d vs. $1/T$ depictions used in obtaining $\Delta H°$ and $\Delta S°$ are significant at $p < 0.01$.

Table 4
Mathematical equation of kinetic models

Model	Equation	Parameters
Pseudo-first-order	$q_t = q_e[1 - e^{-k_1 t}]$	k_1, q_e
Pseudo-second-order	$q_t = \dfrac{t}{\left[\frac{1}{k_2 q_e^2}\right] + \left[\frac{t}{q_e}\right]}$	k_2, q_e
Elovich	$q_t = \frac{1}{b}\ln(ab) + \frac{1}{b}\ln t$	a, b
Intraparticle diffusion	$q_t = k_i t^{0.5}$	k_i

Notes: q_t: The adsorbed amounts at time t (mol kg^{-1}), q_e: The adsorbed amounts at equilibrium (mol kg^{-1}), k_1, k_2, and k_i are the rate constants a: the initial adsorption rate (mol/kg min) b: Related to the extent of surface coverage and the activation energy involved in chemisorption (kg/mol). The constant k_2 (1/h) is the adsorption rate constant of pseudo-first-order reaction. Initial adsorption rate (H) for pseudo-second-order is also calculated from $H = k_2 Q_e^2$.

Table 5
Kinetic parameters for UO_2^{2+} adsorption onto PAA-B-L

	Parameters
Pseudo-first-order kinetic	
[a]q_{cal}	0.223
[b]k	0.038
R^2	0.878
Pseudo-second-order kinetic	
[a]q_{cal}	0.244
[c]k	0.229
[d]H	0.014
[e]$t_{1/2}$	17.89
R^2	0.947
Elovich model	
[f]a	0.024
[g]b	26.96
R^2	0.973
Intraparticle diffusion	
[f]k_i	6.11×10^{-3}
R^2	0.947

Notes: Q_{exp} 0.226 for PAA-B-L (significant at $p < 0.01$ for coefficient of correlation).
[a](mol kg^{-1}).
[b](dk^{-1}).
[c](mol^{-1} kg min^{-1}).
[d](mol kg^{-1} min).
[e](dk).
[f](mol kg^{-1} min^{-1}).
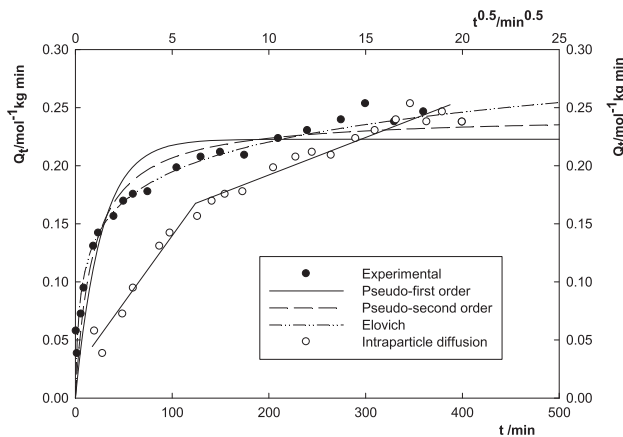[g](kg mol^{-1}).

Fig. 11. Compatibility of UO_2^{2+} adsorption kinetics to pseudo-first-order model, pseudo-second-order model, Elovich model, and intraparticle diffusion model.

3.5. Thermodynamic parameters for adsorption of UO_2^{2+}

Three different temperature points, 283, 298, and 313 K were studied for the determination of thermodynamic parameters of adsorption.

The distribution coefficients (K_d) was derived from:

$$K_d = \frac{Q}{C_e} \tag{2}$$

The free energy of adsorption ($\Delta G°$) is related to K:

$$\Delta G° = -RT \ln K_d \tag{3}$$

The value of enthalpy changes ($\Delta H°$) and entropy changes ($\Delta S°$) for adsorption was calculated using equation in below:

$$\ln K_d = \frac{\Delta S^\circ}{R} - \frac{\Delta H^\circ}{RT} \qquad (4)$$

Thermodynamic parameters were derived from the depictions of "ln K_d vs. $1/T$" (Fig. 10), and (E_{DR}) derived from DR model were provided in Table 3. The ΔH°, ΔS°, and ΔG° values showed that the adsorption is endothermic, entropy increases, and spontaneity is as expected ($\Delta G^\circ < 0$).

The value for ΔH suggests that these processes are endothermic, meaning it consumes energy. In addition, the adsorption of UO_2^{2+} is endothermic, thus the adsorption increases with temperature. If the change of ΔS° value is bigger than -10 J K^{-1} mol^{-1}, this means adsorption reaction is based on dissociative mechanism, otherwise associative mechanism [42]. Our results showed that the overall process occurred through associative mechanism which increased randomness at the system during the adsorption due to some structural changes in the solid and solution [43].

3.6. Effect of time to adsorption of UO_2^{2+}

The prediction of adsorption rate provides important information for designing the adsorption process. Generally, the kinetic of adsorption is described using empirical kinetic equations such as pseudo-first-order, pseudo-second-order [44], intraparticle diffusion [45], and Elovich [46]. All used equations and related parameters are given Table 4 in order to investigate experimental data. Results of kinetic studies and their fitting to equations were evaluated in Fig. 11.

In order to make a correlation between the experimental results, the kinetic equations were evaluated by using non-linear regression coefficient for pseudo-first-order, pseudo-second, Elovich, and linear regression coefficient for intraparticle diffusion. The experimental results are not compatible to the pseudo-first-order model. The best correlations were obtained with pseudo-second-order, Elovich and intraparticle diffusion models. Our results showed that the kinetics of uranyl adsorption on to PAA-B-L could be explained by pseudo-second-order model. This model assumed that the more the values obtained from the experiment (q_{exp}) and the ones obtained from the second-order model (q_{cal}) are close to each other, the more the nature of adsorption is concentration dependent (Table 5).

According to Elovich model, initial adsorption is fast while it is getting slower at later period [47]. Intraparticle diffusion model showed that adsorption behavior of material follows on a different mechanism because the q vs $t^{1/2}$ plot is multi-linear [45]. This behavior can explain that adsorption is fast on external surface at initial period and then it is getting slower at later period because of mass transfer to internal parts. The results showed that the kinetic mechanism of adsorption on to PAA-B-L can be explained using pseudo-second-order, Elovich, and intraparticle diffusion models together.

4. Conclusions

B-PAA-L composite was synthesized and characterized successfully. The adsorption data follow Langmuir, Freundlich, Temkin, and DR isotherms and the maximum adsorption capacities was found as 0.314 mol kg^{-1} for Langmuir. The value of the mean adsorption energy (E_{DR}) was calculated as 11.02 kJ mol^{-1} by providing chemical adsorption nature. The values of ΔH, ΔS and ΔG were calculated as 20.44 kJ mol^{-1}, 109.16 JK^{-1} mol^{-1}, and -12.069 kJ mol^{-1}, respectively.

References

[1] A.P. Gilman, D.C. Villeneuve, V.E. Secours, A.P. Yagminas, B.L. Tracy, J.M. Quinn, V.E. Valli, R.J. Willes, M.A. Moss, Uranyl nitrate: 28-day and 91-day toxicity studies in the Sprague-Dawley rat, Toxicol. Sci. 41 (1998) 117–128.

[2] L.S. Keith, O.M. Faroon, B.A. Fowler, Uranium, in: G.F. Nordberg, B.A. Fowler, M. Nordberg, L. Friberg (Eds.), Handbook on the Toxicology of Metals, Academic Press, Denmark, 2007.

[3] E.A. Santos, A.C. Ladeira, Recovery of uranium from mine waste by leaching with carbonate-based reagents, Environ. Sci. Technol. 45 (2011) 3591–3597.

[4] C. Banerjee, N. Dudwadkar, S.C. Tripathi, P.M. Gandhi, V. Grover, C.P. Kaushik, A.K. Tyagi, Nanocerium vanadate: A novel inorganic ion exchanger for removal of americium and uranium from simulated aqueous nuclear waste, J. Hazard. Mater. 280 (2014) 63–70.

[5] J.C.B.S. Amaral, C.A. Morais, Thorium and uranium extraction from rare earth elements in monazite sulfuric acid liquor through solvent extraction, Miner. Eng. 23 (2010) 498–503.

[6] M.G. Mahfouz, A.A. Galhoum, N.A. Gomaa, S.S. Abdel-Rehem, A.A. Atia, T. Vincent, E. Guibal, Uranium extraction using magnetic nano-based particles of diethylenetriamine-functionalized chitosan: Equilibrium and kinetic studies, Chem. Eng. J. 262 (2015) 198–209.

[7] S. Zhang, X.W. Shu, Y. Zhou, L. Huang, D.B. Hua, Highly efficient removal of uranium (VI) from aqueous solutions using poly(acrylic acid)-functionalized microspheres, Chem. Eng. J. 253 (2014) 55–62.

[8] X. Liu, H. Chen, C. Wang, R. Qu, C. Ji, C. Sun, Y. Zhang, Synthesis of porous acrylonitrile/methyl acrylate copolymer beads by suspended emulsion polymerization and their adsorption properties after amidoximation, J. Hazard. Mater. 175 (2010) 1014–1021.

[9] S. Şimşek, U. Ulusoy, O. Ceyhan, Adsorption of UO_2^{2+}, Tl^+, Pb^{2+}, Ra^{2+} and Ac^{3+} onto polyacrylamide-bentonite composite, J. Radioanal. Nucl. Chem. 256 (2003) 315–321.

[10] S. Şimşek, U. Ulusoy, UO_2^{2+}, Tl^+, Pb^{2+}, Ra^{2+}, Bi^{3+} and Ac^{3+} adsorption onto polyacrylamide-zeolite composite and its modified composition by phytic acid, J. Radioanal. Nucl. Chem. 261 (2004) 79–86.

[11] S. Şimşek, E. Yılmaz, A. Boztuğ, Amine-modified maleic anhydride containing terpolymers for the adsorption of uranyl ion in aqueous solutions, J. Radioanal. Nucl. Chem. 298 (2013) 923–930.

[12] J. Kim, C. Tsouris, Y. Oyola, C.J. Janke, R.T. Mayes, S. Dai, G. Gill, L.J. Kuo, J. Wood, K.Y. Choe, E. Schneider, H. Lindner, Uptake of uranium from seawater by amidoxime-based polymeric adsorbent: Field experiments, modeling, and updated economic assessment, Ind. Eng. Chem. Res. 53 (2014) 6076–6083.

[13] E. Karadağ, Ö.B. Üzüm, S. Kundakci, D. Saraydin, Polyelectrolyte CASA hydrogels for uptake of uranyl ions from aqueous solutions, J. Appl. Polym. Sci. 104 (2007) 200–204.

[14] D. Baybaş, U. Ulusoy, Polyacrylamide–hydroxyapatite composite: Preparation, characterization and adsorptive features for uranium and thorium, J. Solid State Chem. 194 (2012) 1–8.

[15] P. Cakir, S. Inan, Y. Altas, Investigation of strontium and uranium sorption onto zirconium-antimony oxide/polyacrylonitrile (Zr-Sb oxide/PAN) composite using experimental design, J. Hazard. Mater. 271 (2014) 108–119.

[16] T. Koshijima, T. Watanabe, F. Yaku, Structure and properties of the lignin-carbohydrate complex polymer as an amphipathic substance, in: W.G. Glasser, S. Sarkanen (Eds.), Lignin Properties and Materials, 195th National Meeting of the American Chemical Society, Toronto, Canada.

[17] S. Şimşek, D. Baybaş, M.Ç. Koçyiğit, H. Yıldırım, Organoclay modified with lignin as a new adsorbent for removal of Pb^{2+} and UO_2^{2+}, J. Radioanal. Nucl. Chem. 299 (2013) 283–292.

[18] P.M.S.S. Luis, C.Y. Cheng, R.A.R. Boaventura, Adsorption of a basic dye onto esmegel clay, Environ. Eng. Manage. J. 13 (2014) 395–405.

[19] S. Barreca, S. Orecchio, A. Pace, The effect of montmorillonite clay in alginate gel beads for polychlorinated biphenyl adsorption: Isothermal and kinetic studies, Appl. Clay Sci. 99 (2014) 220–228.

[20] U. Ulusoy, S. Şimşek, Ö. Ceyhan, Investigations for modification of polyacrylamide-bentonite by phytic acid and its usability in Fe^{3+}, Zn^{2+} and UO_2^{2+} adsorption, Adsorption 9 (2003) 165–175.

[21] U. Ulusoy, S. Simsek, Lead removal by polyacrylamide-bentonite and zeolite composites: Effect of phytic acid immobilization, J. Hazard. Mater. 127 (2005) 163–171.

[22] H.I. Ulusoy, S. Şimşek, Removal of uranyl ions in aquatic mediums by using a new material: Gallocyanine grafted hydrogel, J. Hazard. Mater. 254–255 (2013) 397–405.

[23] S. Şimşek, U. Ulusoy, Adsorptive properties of sulfolignin–polyacrylamide graft copolymer for lead and uranium: Effect of hydroxilamine–hydrochloride treatment, React. Funct. Polym. 73 (2013) 73–82.

[24] X. Guo, S. Zhang, X.Q. Shan, Adsorption of metal ions on lignin, J. Hazard. Mater. 151 (2008) 134–142.

[25] E. Pretsch, P. Bühlmann, C. Affolter, Structure Determination of Organic Compounds, third ed., Springer, New York, NY, 2000.

[26] H. Yalçin, G. Gümüşer, Mineralogical and geochemical characteristics of late Cretaceous bentonite deposits of the Kelkit Valley Region, northern Turkey, Clay Miner. 35 (2000) 807–825.

[27] S.P. Mun, C.S. Ku, J.P. Kim, Adsorption of metal and uranyl ions onto amidoximated Pinus densiflora bark, Wood Sci. Technol. 44 (2010) 283–299.

[28] G.I. Park, H.S. Park, S.I. Woo, Influence of pH on the adsorption of uranium ions by oxidized activated carbon and chitosan, Sep. Sci. Technol. 34 (1999) 833–854.

[29] R. Guillaumont, T. Fanghanel, V. Neck, J. Fuger, D.A. Palmer, I. Grenthe, M.H. Rand, Update on the chemical thermodynamics of uranium, neptunium, plutonium, americium and technetium, OECD Nuclear Energy Agency, Data Bank Issy-les-Moulineaux, France, 2003.

[30] C.J. Chisholm-Brause, J.M. Berg, R.A. Matzner, D.E. Morris, Uranium(VI) sorption complexes on montmorillonite as a function of solution chemistry, J. Colloid Interface Sci. 233 (2001) 38–49.

[31] L.S. Čerović, S.K. Milonjić, M.B. Todorović, M.I. Trtanj, Y.S. Pogozhev, Y. Blagoveschenskii, E.A. Levashov, Point of zero charge of different carbides, Colloids Surf., A: Physicochem. Eng. Aspects 297 (2007) 1–6.

[32] G. Limousin, J.P. Gaudet, L. Charlet, S. Szenknect, V. Barthès, M. Krimissa, Sorption isotherms: A review on physical bases, modeling and measurement, Applied Geochem. 22 (2007) 249–275.

[33] M.C. Ncibi, Applicability of some statistical tools to predict optimum adsorption isotherm after linear and non-linear regression analysis, J. Hazard. Mater. 153 (2008) 207–212.

[34] N.D. Hutson, R.T. Yang, Theoretical basis for the Dubinin-Radushkevitch (D-R) adsorption isotherm equation, Adsorption 3 (1997) 189–195.

[35] J.E. Shields, S. Lowell, Powder surface area and porosity, second ed., Chapman and Hall, New York, NY, 1984.

[36] O. Hamdaoui, E. Naffrechoux, Modeling of adsorption isotherms of phenol and chlorophenols onto granular activated carbon—Part I. Two-parameter models and equations allowing determination of thermodynamic parameters, J. Hazard. Mater. 147 (2007) 381–394.

[37] A.R. Khataee, F. Vafaei, M. Jannatkhah, Biosorption of three textile dyes from contaminated water by filamentous green algal *Spirogyra* sp.: Kinetic, isotherm and thermodynamic studies, Int. Biodeterior. Biodegrad. 83 (2013) 33–40.

[38] A. Günay, E. Arslankaya, İ. Tosun, Lead removal from aqueous solution by natural and pretreated clinoptilolite: Adsorption equilibrium and kinetics, J. Hazard. Mater. 146 (2007) 362–371.

[39] R.I. Yousef, B. El-Eswed, A.A.H. Al-Muhtaseb, Adsorption characteristics of natural zeolites as solid adsorbents for phenol removal from aqueous solutions: Kinetics, mechanism, and thermodynamics studies, Chem. Eng. J. 171 (2011) 1143–1149.

[40] F. Taghizadeh, M. Ghaedi, K. Kamali, E. Sharifpour, R. Sahraie, M.K. Purkait, Comparison of nickel and/or zinc selenide nanoparticle loaded on activated carbon as efficient adsorbents for kinetic and equilibrium study of removal of Arsenazo (III) dye, Powder Technol. 245 (2013) 217–226.

[41] M.H. Bradbury, B. Baeyens, Sorption of Eu on Na- and Ca-montmorillonites: Experimental investigations and modelling with cation exchange and surface complexation, Geochim. Cosmochim. Acta 66 (2002) 2325–2334.

[42] K.G. Scheckel, D.L. Sparks, Temperature effects on nickel sorption kinetics at the mineral–water interface, Soil Sci. Soc. Am. J. 65 (2001) 719–728.

[43] D. Mohan, K.P. Singh, G. Singh, K. Kumar, Removal of dyes from wastewater using flyash, a low-cost adsorbent, Ind. Eng. Chem. Res. 41 (2002) 3688–3695.

[44] Y.S. Ho, G. McKay, Pseudo-second order model for sorption processes, Process Biochem. 34 (1999) 451–465.

[45] W.H. Cheung, Y.S. Szeto, G. McKay, Intraparticle diffusion processes during acid dye adsorption onto chitosan, Bioresour. Technol. 98 (2007) 2897–2904.

[46] S. Sen Gupta, K.G. Bhattacharyya, Kinetics of adsorption of metal ions on inorganic materials: A review, Adv. Colloid Interface Sci. 162 (2011) 39–58.

[47] B.J. Liu, Q.L. Ren, Sorption of levulinic acid onto weakly basic anion exchangers: Equilibrium and kinetic studies, J. Colloid Interface Sci. 294 (2006) 281–287.